Mass loss of Greenland's glaciers and ice caps 2003-2008 revealed from ICESat laser altimetry data

Bolch, Tobias ; Sandberg Sørensen, L ; Simonsen, S B ; Mölg, Nico ; Machguth, Horst ; Rastner, Philipp ; Paul, Frank

DOI: https://doi.org/10.1002/grl.50270

Mass loss of Greenland's glaciers and ice caps 2003–2008 revealed from ICESat laser altimetry data

T. Bolch,[1,2] L. Sandberg Sørensen,[3] S. B. Simonsen,[4,5] N. Mölg,[1] H. Machguth,[1,6] P. Rastner,[1] and F. Paul[1]

Received 28 November 2012; revised 13 February 2013; accepted 18 February 2013; published 13 March 2013.

[1] The recently finalized inventory of Greenland's glaciers and ice caps (GIC) allows for the first time to determine the mass changes of the GIC separately from the ice sheet using space-borne laser altimetry data. Corrections for firn compaction and density that are based on climatic conditions are applied for the conversion from volume to mass changes. The GIC which are clearly separable from the icesheet (i.e., have a distinct ice divide or no connection) lost 27.9 ± 10.7 Gt a^{-1} or 0.08 ± 0.03 mm a^{-1} sea-level equivalent (SLE) between October 2003 and March 2008. All GIC (including those with strong but hydrologically separable connections) lost 40.9 ± 16.5 Gt a^{-1} (0.12 ± 0.05 mm a^{-1} SLE). This is a significant fraction (~14 or 20%) of the reported overall mass loss of Greenland and up to 10% of the estimated contribution from the world's GIC to sea level rise. The loss was highest in southeastern and lowest in northern Greenland.
Citation: Bolch, T., L. Sandberg Sørensen, S. B. Simonsen, N. Mölg, H. Machguth, P. Rastner, and F. Paul (2013), Mass loss of Greenland's glaciers and ice caps 2003–2008 revealed from ICESat data, *Geophys. Res. Lett.*, *40*, 875–881, doi:10.1002/grl.50270.

1. Introduction

[2] Glaciers and ice caps (GIC) are key indicators of climate change [e.g., *Lemke et al*., 2007], and their melt water could potentially make a substantial contribution to sea-level rise (SLR) during this century [*Meier et al*., 2007]. This is especially true for the GIC in Greenland which cover an area of about 89,000 km^2 when considering only ice bodies that are not or only weakly connected to the ice sheet [*Rastner et al*., 2012]. This area is up to twice as large as previously estimated (e.g., *Weidick and Morris*, 1998; *Radic and Hock*, 2010]) and comprises about 12% of the global GIC area as recorded in the Randolph Glacier Inventory [*Arendt et al*., 2012].

[3] A large number of studies have estimated the overall mass budget for Greenland (ice sheet including GIC to a varying degree) based on Gravity Recovery and Climate Experiment (GRACE) data (e.g., [*Velicogna*, 2009; *van den Broeke et al*., 2009]), altimetry data (e.g., [*Sørensen et al*., 2011; *Pritchard et al*., 2009]), or mass balance modeling [*Ettema et al*., 2009]. However, the contribution of the GIC alone has not been assessed so far despite their potentially high contribution to SLR. This was largely a consequence of a missing detailed glacier inventory that is needed to determine the GIC contribution precisely. The new inventory [*Rastner et al*., 2012] allowed us also to investigate the marine-terminating and land-terminating glaciers separately. The mass changes of the latter are a direct reaction to climate forcing while the interaction with the ocean alters the signal of the former.

[4] Existing mass balance studies on individual glaciers, such as Mittivakkat Glacier in southeast Greenland, suggest that glaciers are shrinking and losing mass [*Mernild et al*., 2011] like in most other parts of the world [*WGMS*, 2008] and that the majority of the non-surge-type glaciers continued to retreat during the last decades [*Bjørk et al*., 2012; *Citterio et al*., 2009; *Leclercq et al*. 2012] with larger retreats for the marine-terminating glaciers [*Jiskoot et al*., 2012]. However, altimetry data also revealed that Greenland's largest ice cap Flade Isblink (located in the north-east) had a mass budget close to zero [*Rinne et al*., 2011]. There is thus some spatial variability to be expected that can be determined from the Ice, Cloud, and land Elevation Satellite (ICESat) altimetry dataset. Here we report the elevation changes over the October 2003 to March 2008 period for the GIC on Greenland based on processed ICESat data [cf. *Sørensen et al*., 2011] and the new GIC inventory [*Rastner et al*., 2012]. Our focus is on the regional variability, a differentiation between marine and land-terminating glaciers, and an adequate consideration of firn compaction and density differences.

2. Data and Methods

2.1. Glacier Data

[5] The utilized glacier outlines were mainly derived semi-automatically from more than 70 Landsat Enhanced Thematic Mapper (ETM)+ scenes with a focus on the years 1999 to 2002 and the Greenland Ice Mapping Project (GIMP) digital elevation model (DEM) [*Rastner et al*., 2012]. The area north of the Landsat coverage (~80°N)

All Supporting Information may be found in the online version of this article.

[1]Department of Geography, University of Zurich, Winterthurer Str. 190, 8057, Zürich, Switzerland.
[2]Institute for Cartography, Technische Universität Dresden, 01069, Dresden, Germany.
[3]Geodynamics Department, DTU Space, Elektrovej, Building 328, 2800 Kgs. Lyngby, Denmark.
[4]Centre for Ice and Climate, NBI, University of Copenhagen, Juliane Maries Vej 30, 2100, Copenhagen, Denmark.
[5]Danish Climate Centre, DMI, Lyngbyvej 100, 2100, Copenhagen, Denmark.
[6]Geological Survey of Denmark and Greenland (GEUS), Voldgade 10, 1350, Copenhagen, Denmark.

T. Bolch, Department of Geography, University of Zurich, Winterthurer Str. 190, 8057 Zürich, Switzerland. (tobias.bolch@geo.uzh.ch)

0094-8276/13/10.1002/grl.50270

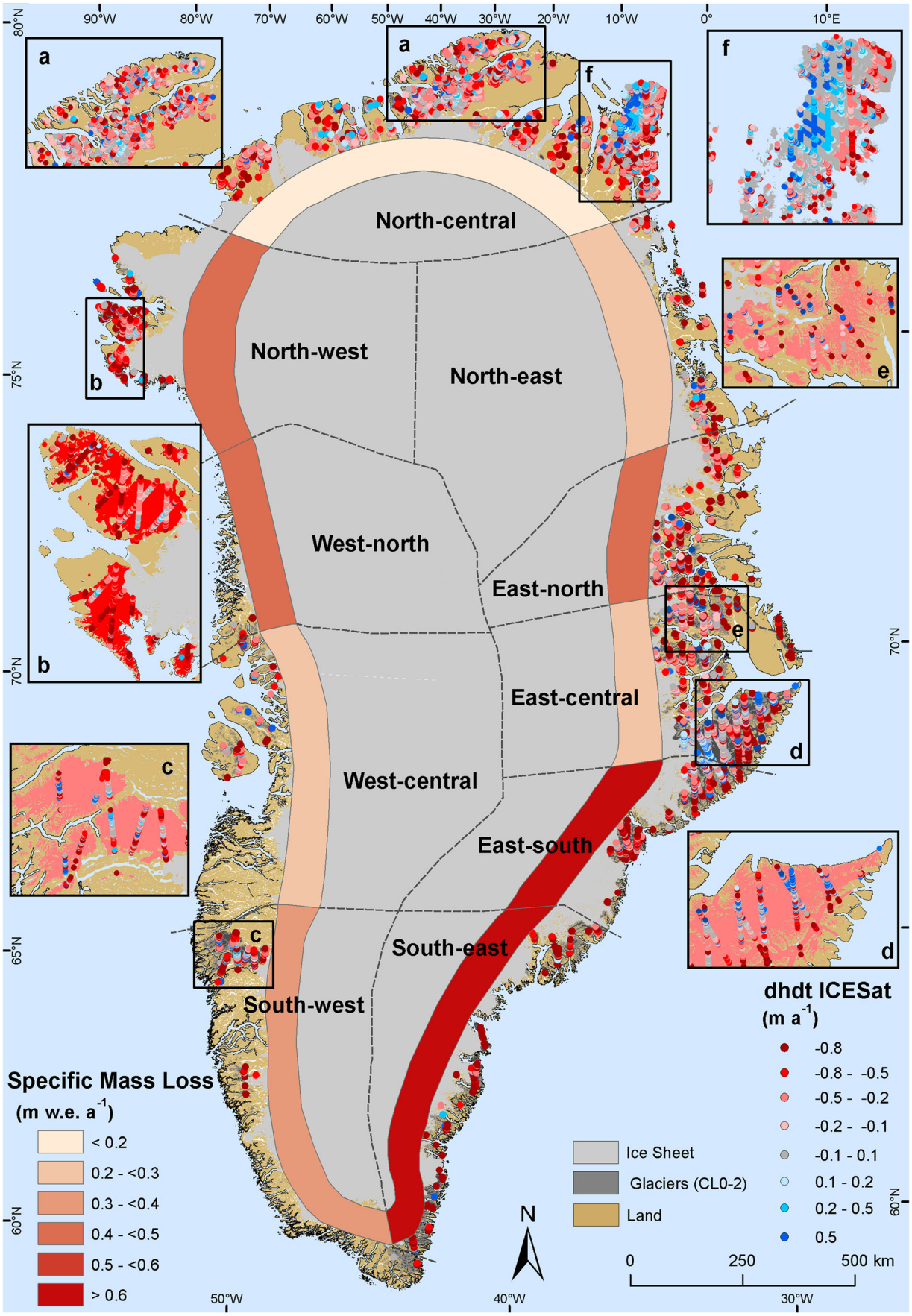

Figure 1. Mean mass changes for the 10 sectors and elevation changes for the GIC derived from ICESat points. The color of the GIC in the insets a–f represents the mean elevation change according to the legend for dh/dt ICESat.

was filled with the GIMP ice cover map (http://bprc.osu.edu/GDG/icemask.php) that was further adjusted with Moderate Resolution Imaging Spectroradiometer (MODIS) data. The inventory distinguishes three levels of connectivity to the ice sheet: CL0 has no connection to the ice sheet, CL1 has a weak connection, and CL2 has a strong connection to the ice sheet but is still hydrologically separable [*Rastner et al*., 2012]. The ice-covered area is ~89,000 km^2 for CL0 and CL1 and ~130,000 km^2 when including also CL2 areas. Here we present results separately for all GIC (CL0, 1, and 2) and those which are clearly separable from the ice sheet (CL0 and CL1). We divided Greenland in four major regions (north, east, south, and west) and 10 sectors (Figure 1) following *Rastner et al*. [2012] to derive a differentiated picture of the regional mass changes. All values are calculated and averaged for these sectors. The glacier hypsometry was derived from the GIMP DEM (http://bprc.osu.edu/GDG/gimpdem.php).

2.2. ICESat

[6] The elevation change data were obtained from the ICESat Geoscience Laser Altimeter System (GLAS) which was launched in January 2003. The laser system was operating at a wavelength of 1064 nm with footprints of about 70 m and a sampling frequency of about 170 m along track [*Zwally et al*., 2002]. The tracks are separated horizontally by ~30 km in southern and ~10 km in northern Greenland. The elevation changes are based on ICESat GLA12 data (release 531) and represent the mean of the time period from October 2003 to March 2008, taking into account all of the data available in this period. We performed the following data culling and correction procedures to reduce systematic errors and outliers (cf. [*Sørensen et al*., 2011], method M3, for full details): (a) a saturation correction to reduce elevation estimation errors originating from the saturation of the waveform as to reduce systematic errors in the measurements, (b) identification of thresholds of the so-called IceSvar parameter—showing the difference between the return signal and a Gaussian functional fit—to reject data with a large misfit (cf. [*Smith et al*., 2009]), and (c) identification and elimination of data with multiple peaks. The mean elevation change is derived by assuming that within 500 m the ice surface elevation can be represented by a rigid plane that varies linearly with time. A sine and cosine term describes the seasonal changes, which were consequently separated from the mean annual elevation change. The mean surface elevation changes were estimated at 500 m along track resolution and associated with variance from the regression procedure (cf. [*Sørensen et al*., 2011]). In addition, we assume that the error within each 500 m segment remains constant and, hence, the variances should reflect both the error of the measurements and the accuracy of the fit. For utilization of this dataset to the GIC and also to better approximate the assumption of a rigid plane, only data points lying at >250 m from the glacier margin are considered (glacier surfaces are usually having more constant slopes than the surroundings). Further filtering of the data is applied by rejecting implausibly high dh/dt values (>10 ma^{-1}), which corresponds roughly to

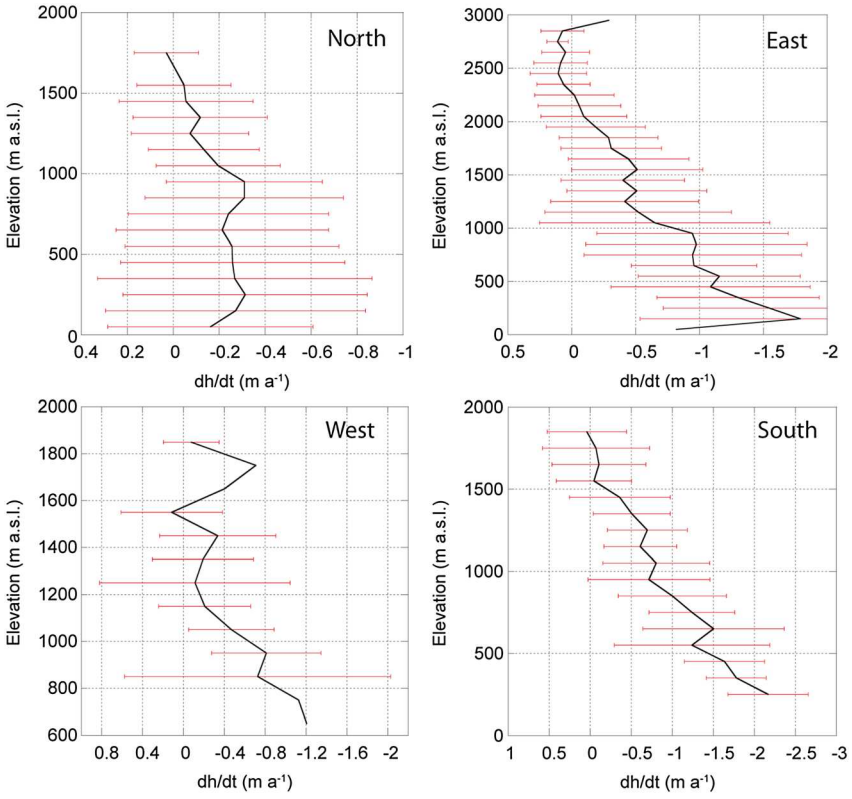

Figure 2. Mean annual elevation changes from 2003 to 2008 in 100 m bins vs. mean elevation for the four major regions as derived from the ICESat measurements. The red bars indicate the standard deviation for each interval but are only shown in case five or more ICESat measurements are available.

the highest/lowest 2.5% of the data. In addition, data points with high variances from the linear regression procedure (>1.0) were eliminated. In total 27,799 out of 40,475 data points were selected for elevation change analysis.

[7] The density of the ICESat points is large in the north (>20,000 ICESat points) so that most of the GIC are well covered, while the distance between tracks reaches about 30 km in the south and results in a low number of glaciers with sufficient coverage (~1750 points). We compared therefore the area-elevation distribution of the ICESat data points with the hypsometry for all glaciers in each sector as derived from the GIMP DEM (Figure S1 in Supporting Information). The deviation is for most altitudes and regions within ±10% with the highest deviation (+22%) occurring at elevations of about 1250 m a.s.l. in the western sectors. However, the lowest elevations, where most of the surface lowering occurred (except for the north, Figure 2), are well covered. To quantify the uncertainties due to varying track and thus point densities, we (a) randomly choose 50% of the points and (b) selected every second ICESat track. The deviations were around 4% for (a) and 5.5% for (b) with a maximum of 8% in Greenland's middle and middle-to-south latitudes. These values were considered in the uncertainty analysis. In order to estimate the volume loss for all GIC, we used the calculated along-track dh/dt-curves and applied them to the whole GIC area using the area-elevation distribution. The R^2 for the regression of dh/dt against elevation was up to 0.44 (east-south) but was low for sectors showing no clear trend with altitude (south-west, west, and north). For these sections, we calculated the elevation changes based on the mean dh/dt of all points below and above the ELA. This procedure was also performed for comparison and uncertainty estimation. The differences between these two procedures are about ±7% for most of the sections and highest (±25%) for the south-west section.

2.3. Density Determination

[8] Snow, firn, and ice densities and firn compaction must be taken into account when converting elevation changes into mass changes. We calculated the firn density based on an empirical relationship between snow density and mean firn temperature (at 10 m depth based on the mean annual air temperature, MAAT) by *Reeh et al*. [2005]. The MAAT is calculated as a function of surface elevation and geographical position according to *Fausto et al*. [2009]. The MAAT and the resulting firn density are derived for each sector. The dh/dt values above the equilibrium line altitude (ELA) are multiplied by the regional firn density and the values below the ELA are multiplied by the typical density of glacier ice (900 kg/m^3), resulting in average regional values between 528 kg m^{-3} (north-west sector) and 796 kg m^{-3} (east-south sector) (cf. Tables *S1* and *S2*). The ELA is approximated by the median elevation of each glacier (cf. [*Braithwaite and Raper*, 2009]). We estimate the uncertainty based on one standard deviation and assume that the uncertainty due to the rough estimate of the ELA is also considered by this conservative estimate of ±150 kg m^{-3}.

[9] The derivation of the firn compaction follows *Sørensen et al*. [2011], where the change in the air space of the top firn (top 15 annual layers) is estimated from a dynamic firn model based on the description of firn compaction by *Herron and Langway* [1980] and *Arthern et al*. [2010]. The dynamical firn model is forced by interpolated output fields from the HIRHAM5 regional climate model at a resolution of 5 × 5 km [*Lucas-Picher et al*., 2012]. The retention of melt water in the firn pack is assumed to be confined to the surface layer formed in the same period of time as the melt [*Reeh*, 2008]. The resolution of the model is too low to address each glacier individually, but it provides reasonable results for each sector. We estimated the uncertainty from the error in the linear fit of the interannual variability of the firn column and conservatively assumed the higher estimate of ~7.5% of the total mass change [cf. *Sørensen et al*., 2011]. The results revealed a mean change in firn densification of about -0.05 ± 0.01 m a^{-1} with the highest value in the warmer and wetter east-south sector (-0.22 m ± 0.02 m a^{-1}) and a slight expansion in the cold and dry north ($+0.09 \pm 0.01$ m a^{-1}) (Tables S1, S2).

[10] The potential overall uncertainty of the mass budget calculations is manifold and comprises especially the uncertainty in ICESat data itself (e_{ICESat}), the spatial interpolation of the ICESat samples (e_{Interp}), the density assumption (e_{Dens}), and the firn compaction model (e_{Firn}). Assuming that the sources are independent the total uncertainty would be as follows:

Table 1. Statistics and Derived Mass Changes for the GIC on Greenland that are Clearly Separable from the Ice Sheet (CL0, CL1)

	Land Terminating GIC Only				All GIC Including Marine Terminating			
Sector	Area (km^2)	Nr. points	Mean dh (m a^{-1})	Mass change (Gt a^{-1}]	Area (km^2)	Nr. points	Mean dh (m a^{-1})	Mass change (Gt a^{-1})
East-north	8,462	1,162	−0.61	−3.5 ± 1.5	8,795	1,191	−0.63	−3.8 ± 1.6
East-central	11,905	1,415	−0.40	−3.3 ± 1.4	13,757	3,104	−0.40	−3.9 ± 1.6
East-south	1,045	23	−0.86	−0.6 ± 0.2	3,080	1,352	−0.96	−2.2 ± 0.8
East total	21,411	2,600	*−0.50*	−7.4 ± 3.1	25,631	5,697	*−0.55*	−9.9 ± 4.0
South-east	2,354	68	−1.30	−2.2 ± 0.9	7,056	511	−1.37	−7.0 ± 2.9
South-west	5,481	560	−0.45	−2.1 ± 0.9	8,492	732	−0.43	−3.3 ± 1.4
South total	7,835	628	*−0.75*	−3.3 ± 1.8	15,548	1,243	*−0.90*	−10.3 ± 4.2
West-central	4,773	275	−0.28	−1.0 ± 0.4	5,045	285	−0.28	−1.0 ± 0.4
West-north	722	41	−0.77	−0.3 ± 0.1	729	42	−0.77	−0.4 ± 0.1
West total	5,495	316	*−0.35*	−1.3 ± 0.5	5,775	327	*−0.35*	−1.4 ± 0.5
North-west	2,699	797	−0.60	−1.1 ± 0.4	4,340	849	−0.60	−1.8 ± 0.7
North-central	18,116	7,788	−0.28	−3.8 ± 1.6	34,992	8,192	−0.18	−3.9 ± 1.7
North-east	2,667	580	−0.27	−0.5 ± 0.2	3,039	661	−0.29	−0.6 ± 0.3
North total	23,482	9,166	*−0.33*	−5.3 ± 1.8	42,370	9,702	*−0.23*	−6.30 ± 2.23
Total	*58,223*	*12,708*	**−0.45**	*−18.5* ± 7.2	*89,324*	*17,009*	**−0.45**	*−27.9 ± 10.7*

Table 2. Statistics and Derived Mass Changes for the GIC on Greenland (CL0–Cl2)

	Land Terminating GIC Only				All GIC Including Marine Terminating			
Sector	Area (km^2)	Nr. points	Mean dh ($m\ a^{-1}$)	Mass change ($Gt\ a^{-1}$)	Area (km^2)	Nr. points	Mean dh ($m\ a^{-1}$)	Mass change ($Gt\ a^{-1}$)
East-north	10,038	1,338	−0.58	-3.9 ± 1.7	10,371	1,367	−0.60	-4.2 ± 1.8
East-central	15,075	1,819	−0.38	-4.0 ± 1.6	33,955	4,923	−0.38	-9.4 ± 3.9
East-south	1,294	29	−0.83	-0.7 ± 0.2	14,004	1,381	−0.67	-6.6 ± 2.4
East total	26,408	3,186	*−0.47*	-8.6 ± 3.5	58,330	7,671	*−0.48*	-20.3 ± 8.0
South-east	3,026	133	−1.23	-2.7 ± 1.1	12,114	645	−1.32	-11.3 ± 4.6
South-west	5,790	574	−0.45	-1.8 ± 0.7	8,843	746	−0.43	-3.4 ± 1.4
South total	8,816	708	*−0.76*	-4.4 ± 1.9	20,957	1,391	*−0.96*	-14.7 ± 6.0
West-central	4,919	279	−0.27	-0.9 ± 0.4	5,258	289	−0.28	-1.0 ± 0.4
West-north	765	41	−0.77	-0.4 ± 0.1	772	41	−0.77	-0.4 ± 0.1
West total	5,684	320	*−0.34*	-1.3 ± 0.5	6,030	330	*−0.34*	-1.4 ± 0.5
North-west	3,051	917	−0.62	-1.3 ± 0.5	6,368	1,766	−0.68	-2.9 ± 1.2
North-central	18,182	7,788	−0.28	-3.9 ± 1.7	35,059	15,980	−0.18	-3.9 ± 1.7
North-east	2,922	580	−0.27	-0.6 ± 0.2	3,294	661	−0.29	-0.7 ± 0.3
North total	24,155	9,285	*−0.33*	-4.4 ± 1.9	44,721	18,407	*−0.26*	-4.5 ± 1.9
Total	65,062	13,499	**−0.45**	-18.8 ± 7.9	130,037	27,799	**−0.48**	-40.9 ± 16.5

$$e = \sqrt{e^2_{ICESat} + e^2_{Interp} + e^2_{Dens} + e^2_{Firn}}. \quad (1)$$

[11] The accuracy of the ICESat elevation data is in the ideal case over flat terrain ±0.15 m, but still sufficiently accurate over glaciers and ice caps (about ±0.5 m, *Moholdt et al*. [2010]). Another uncertainty to consider, although small, is the ICESat intercampaign bias. We assume similar values ($-0.013\ m\ a^{-1}$) for our data as calculated by *Sørensen et al*. [2011]. Hence, the estimated overall uncertainty of the ICESat data is $0.113\ m\ a^{-1}$. We did not explicitly correct the dh/dt for bedrock movement caused by glacio-istostatic adjustment, but assume that this is included in this conservative uncertainty estimate.

3. Results

[12] The GIC in Greenland showed a mean surface lowering of around $0.45\ m\ a^{-1}$ for the period October 2003–March 2008 (Tables 1 and 2), resulting in an overall volume loss of about $40\ km^3\ a^{-1}$ for the CL0 and CL1 glaciers and about $60\ km^3\ a^{-1}$ for all local GIC. The resulting mass loss for the CL0 and CL1 glaciers is $27.9 \pm 10.7\ Gt\ a^{-1}$, corresponding to $0.08 \pm 0.03\ mm\ a^{-1}$ SLE but only $18.5 \pm 7.2\ Gt\ a^{-1}$, when excluding marine-terminating glaciers. This large difference can mainly be explained by the large overall area of marine-terminating glaciers (~31,000 km^2 or 34.5% of all GIC). The overall ice loss of all Greenland GIC was $40.9 \pm 16.5\ Gt\ a^{-1}$ ($0.12 \pm 0.05\ mm\ a^{-1}$ SLE).

[13] The mass loss is not homogeneously distributed, but differs substantially among the regions (Figure 1). The highest average specific mass loss (average loss per unit area) for CL0 and CL1 glaciers occurred in the southeastern sector ($1.0 \pm 0.3\ m\ w.e.\ a^{-1}$) while the loss was lowest in the north-central sector ($0.1 \pm 0.05\ m\ w.e.\ a^{-1}$). The overall pattern of the regional mass change of all GIC is similar to those with CL0 and CL1. Overall, the total mass loss from marine and land-terminating glaciers is similar with a mean specific mass loss of $0.34\ m\ w.e.\ a^{-1}$. The largest contribution to the mass loss of marine-terminating glaciers with CL2 connectivity can be found in the south-east sector (~4 $Gt\ a^{-1}$), and the glaciers in the east, dominated by the Geikie Plateau, which adds another ~3 $Gt\ a^{-1}$. Somewhat special is Flade Isblink, the largest ice cap of Greenland (~7500 km^2) which is also marine-terminating (Figure 1f): It showed no mass loss at its northeastern margins and had an overall mass budget of about zero in close agreement with *Rinne et al*. [2011]. Other large ice caps like Sukkertoppen (West, Figure 1c) and Washington Land (North-central sector) had a clearly negative budget.

4. Discussion and Conclusions

[14] We applied ICESat data to estimate volume changes for Greenland's GIC after a rigorous quality check and several adjustments. The major problem is the large distance between the ICESat tracks especially in the southern sectors. Nevertheless, the ICESat points represent the hypsography of the glaciers quite well (Figure S1) and the observed surface lowering is significant even when assigning high-uncertainty ranges.

[15] We considered both the density of firn and ice and, in contrast to other studies which applied ICESat data on GIC (e.g., [*Gardner et al*., 2010; *Moholdt et al*., 2010; *Kääb et al*., 2012]), also the firn compaction for the conversion of volume to mass changes. The resolution of the compaction model is too coarse for individual glaciers but provided reasonable results and reflects the expected general pattern, e.g., high densification in the wetter and warmer south-east and little densification in the dryer and colder north. The applied dh corrections account for up to ¼ of the ICESat-derived elevation changes in the accumulation area and alter the overall volume changes by ~15% and are hence important to consider (cf. *Sørensen et al*. [2011]). However, these corrections are within the overall uncertainty range. Our estimated firn and ice densities are more at the lower bound. Taking estimates for glaciers like $600\ kg\ m^{-3}$ for the accumulation and $900\ kg\ m^{-3}$ for the ablation area used in other studies (cf. *Gardner et al*. [2010]) would result in a mass loss of $31.3\ Gt\ a^{-1}$ for all CL0 and CL1 glaciers, i.e., $3.5\ Gt\ a^{-1}$ larger than our estimate.

[16] The total and specific mass losses from marine and land-terminating glaciers are similar although one might expect a higher loss of the former due to enhanced melt from ice-water interaction and calving. This might be explained by the usually larger accumulation area at high elevations with slight mass gains (see insets in Figure 1), which offsets the higher mass loss at the tongues. *Gardner et al*. [2010] found a similar pattern for the Canadian Arctic. The specific mass

budget of about zero of the calving glaciers in the northern section in comparison to a mass budget of -0.20 m w.e. a^{-1} of the other glaciers is mainly caused by the Flade Isblink. In-situ mass balance measurements of Mittivakkat Glacier in the southeast, the only one with longer-term data, revealed a mean mass loss of ~0.82 m w.e. a^{-1} for 2003–2008 [*Mernild et al*., 2011] which is within the range of our results for the south-east sector (-1.0 ± 0.3 m w.e. a^{-1}).

[17] The mass loss of the Greenland ice sheet according to different methods is slightly higher than 200 Gt a^{-1} for a similar period as investigated here [*Schrama et al*., 2011; *Rignot et al*., 2011]. In general, these studies do not clearly separate between GIC and ice sheet, so it is difficult to determine if GIC are included in the estimates. Apart from the formerly missing inventory, this is also due to the coarse resolution of the mass change estimates from GRACE (e.g., [*Velicogna*, 2009]) which do not resolve individual glaciers. Assuming a 200 Gt a^{-1} loss for all of Greenland, the CL0 and CL1 GIC contributed ~14% to the loss, while this would amount to 20% when considering also the CL2 GIC. Hence, the specific mass loss of the GIC is about 2.5 times higher than for the ice sheet as the GIC area (CL0-CL2) is only about 7% of the area of the ice sheet (~1,680,000 km^2, *Rastner et al*. [2012]).

[18] The regional pattern of the GIC mass loss seems to be similar for the ice sheet [*Schrama et al*., 2011]. Most negative mass budgets are found in the southeastern sectors and only limited change is found in the northern sector (Figure 1). Interestingly, the highest mass loss takes place in regions which receive most precipitation and vice versa. Hence, it might be possible that mass changes are correlated to mean annual precipitation amounts. However, further investigations of this hypothesis are needed for clarification.

[19] The obtained mass loss of Greenland's GIC is higher than from the glaciers on Svalbard (4.3 Gt a^{-1} [*Moholdt et al*., 2010]) and in the Russian Arctic (9.1 ± 2.0 Gt a^{-1} [*Moholdt et al*., 2012]), but lower than in the Canadian Arctic Archipelago (61 ± 7 Gt a^{-1} [*Gardner et al*., 2010]). However, the ice-covered area in the latter region is with ~148,000 km^2 significantly larger, yielding a mean specific mass budget of -0.41 ± 0.05 m w.e. a^{-1}. The mass loss for all Greenland GIC (CL0-CL2) is 40.9 ± 16.5 Gt a^{-1} resulting in a less negative specific mass budget of -0.31 ± 0.12 m w.e. a^{-1}.

[20] The published estimates of the contribution of the world's GIC to the sea level rise in the early 21st century vary around 1 mm a^{-1} (e.g., 0.95 mm a^{-1} for 2002–2006 [*Dyurgerov*, 2010], 1.12 mm a^{-1} during 2001–2005 [*Cogley*, 2009]). In this regard, the contribution revealed here for the GIC on Greenland (0.12 ± 0.05 mm a^{-1} for all GIC and 0.08 ± 0.03 mm a^{-1} for the GIC with CL0 and CL1) is significant.

[21] **Acknowledgments.** This work was supported by funding from the ice2sea program from the European Union 7th framework program, grant 226375. Ice2sea contribution 136. F.P. and N.M. acknowledge the funding by the ESA project Glaciers_cci (4000101778/10/I-AM). H.M. acknowledges funding from the Programme for Monitoring of the Greenland Ice Sheet (PROMICE).

References

Arendt, A., et al. (2012), Randolph Glacier Inventory, 2.0: A dataset of global glacier outlines, Global Land Ice Measurements from Space, Boulder Colorado, USA. Digital Media.

Arthern, R. J., D. G. Vaughan, A. M. Rankin, R. Mulvaney, and E. R. Thomas (2010), In situ measurements of Antarctic snow compaction compared with predictions of models. *J. Geophys. Res. (Earth Surface) 115*, F03011. doi:10.1029/2009JF001306.

Bjørk, A. A., K. H. Kjær, N. J. Korsgaard, S. A. Khan, K. K. Kjeldsen, C. S. Andresen, J. E. Box, N. K. Larsen, and S. Funder (2012), An aerial view of 80 years of climate-related glacier fluctuations in southeast Greenland, *Nature Geosci. 5*(6), 427–432.

Braithwaite, R., and S. Raper (2009), Estimating equilibrium-line altitude (ELA) from glacier inventory data, *Ann. Glaciol. 50*(53), 127–132.

Citterio, M., F. Paul, A. P. Ahlstrøm, H. F. Jepsen, and A. Weidick (2009), Remote sensing of glacier change in West Greenland: Accounting for the occurrence of surge-type glaciers, *Ann. Glaciol. 50*(53), 70–80.

Cogley, J. (2009), Geodetic and direct mass-balance measurements: Comparison and joint analysis, *Ann. Glaciol. 50*, 96–100.

Dyurgerov, M. B. (2010), Reanalysis of glacier changes: From the IGY to the IPY, 1960–2008, *Data of Glaciological Studies 108*, 1–116.

Ettema, J., van den Broeke M. R., E. van Meijgaard, W. J. van de Berg, J. L. Bamber, J. E. Box, and R. C. Bales (2009), Higher surface mass balance of the Greenland ice sheet revealed by highresolution climate modeling, *Geophys. Res. Lett. 36*, L12501, doi:10.1029/2009GL038110.

Fausto, R. S., A. P. Ahlstrøm, D. van As, C. E. Bøggild, and S. J. Johnson (2009), A new present-day temperature parameterization for Greenland, *J. Glaciol. 55*(189), 95–105.

Gardner, A. S., G. Moholdt, B. Wouters, G. J. Wolken, D. O. Burgess, M. J. Sharp, C. Cogley, C. Braun, and C. Labine (2010), Sharply increased mass loss from glaciers and ice caps in the Canadian Arctic Archipelago, *Nature 473*, 357–460.

Herron, M. M., and C. C. Langway (1980), Firn densification: An empirical model. *J. Glaciol. 25* (93), 373–385.

Jiskoot, H., D. Juhlin, H. St Pierre, and M. Citterio (2012), Tidewater glacier fluctuations in central East Greenland coastal and fjord regions (1980s–2005), *Ann. Glaciol. 53*(60), 35–44.

Kääb, A., E. Berthier, C. Nuth, J. Gardelle, and Y. Arnaud (2012), Contrasting patterns of early twenty-first-century glacier mass change in the Himalayas, *Nature*, *488*(7412), 495–498.

Leclercq, P. W., A. Weidick, F. Paul, T. Bolch, M. Citterio, and J. Oerlemans (2012), Historical glacier length changes in West Greenland, *Cryosphere 6*, 1339–1343.

Lemke, P., et al. (2007), Observations: Changes in snow, ice and frozen ground, in *Climate Change 2007: The Physical Science Basis. Contribution of Working Group I to the Fourth Assessment Report of the Intergovernmental Panel on Climate Change* edited by S. Solomon, D. Qin, M. Manning, C. Chen, M. Marquis, K.B. Averyt, M. Tignor, and H.L. Miller, 337–384, Cambridge University Press, Cambridge.

Lucas-Picher, P., M. Wulff-Nielsen, J. H. Christensen, G. Aðalgeirsdóttir, R. Mottram, and S. B. Simonsen (2012), Very high resolution regional climate model simulations over Greenland: Identifying added value, *J. Geophys. Res.*, *117*, D02108, doi:10.1029/2011JD016267.

Meier, M. F., M. B. Dyurgerov, U. K. Rick, S. O'Neel, W. T. Pfeffer, R. S. Anderson, S. P. Anderson, and A. F. Glazovsky (2007), Glaciers dominate eustatic sea-level rise in the 21st century, *Science 317*(5841), 1064–1067.

Mernild, S. H., N. T. Knudsen, W. H. Lipscomb, J. C. Yde, J. K. Malmros, B. Hasholt, and B. H. Jakobsen (2011), Increasing mass loss from Greenland's Mittivakkat Gletscher, *Cryosphere 5*(2), 341–348.

Moholdt, G., C. Nuth, J. O. Hagen, and J. Kohler (2010), Recent elevation changes of Svalbard glaciers derived from ICESat laser altimetry, *Remote Sens. Environ. 114*, 2756–2767.

Moholdt, G., B. Wouters, and A. S. Gardner (2012), Recent mass changes of glaciers in the Russian High Arctic, *Geophys. Res. Lett. 39*(10). doi: 10.1029/2012GL051466.

Pritchard, H. D., R. J. Arthern, D. G. Vaughan, and L. A. Edwards (2009), Extensive dynamic thinning on the margins of the Greenland and Antarctic ice sheets, *Nature 461*, 971–975.

Radic, V., and R. Hock (2010), Regional and global volumes of glaciers derived from statistical upscaling of glacier inventory data, *J. Geophys. Res. 115*, F01010. doi:10.1029/2009JF001373

Rastner, P., Bolch, T., Mölg, N., Machguth, H., Le Bris, R., and Paul, F. (2012), The first complete inventory of the local glaciers and ice caps on Greenland. *Cryosphere 6*, 1483–1495.

Reeh, N. (2008), A nonsteady-state firn-densification model for the percolation zone of a glacier. *J. Geophys. Res. 113*. doi:10.1029/ 2007JF000746.

Reeh, N., D. A. Fisher, R. M. Koerner, and H. B. Clausen (2005), An empirical firn-densification model comprising ice lenses, *Ann. Glaciol. 42*, 101–106.

Rignot, E., I. Velicogna, M. R. van den Broeke, A. Monaghan, and J. Lenaerts (2011), Acceleration of the contribution of the Greenland and Antarctic ice sheets to sea level rise, *Geophys. Res. Lett*. 38(5). doi: 10.1029/2011GL046583.

Rinne, E., A. Shepherd, S. Palmer, M. van den Broeke, A. Muir, J. Ettema, and D. Wingham (2011), On the recent elevation changes at the Flade Isblink Ice Cap, northern Greenland, *J. Geophys. Res. 116*. F03024, doi:10.1029/2011JF001972.

Schrama, E., B. Wouters, and B. Vermeersen (2011), Present Day Regional Mass Loss of Greenland Observed with Satellite Gravimetry, *Surv. Geophys. 32*(4–5), 377–385.

Smith, B. E., H. A. Fricker, I. R. Joughin, and S. Tulaczyk (2009), An inventory of active subglacial lakes in Antarctica detected by ICESat (2003–2008), *J. Glaciol. 55*(192), 573–595.

Sørensen, L. S., S. B. Simonsen, K. Nielsen, P. Lucas-Picher, G. Spada, G. Adalgeirsdottir, R. Forsberg, and C. S. Hvidberg (2011), Mass balance of the Greenland ice sheet (2003–2008) from ICESat data–the impact of interpolation, sampling and firn density, *Cryosphere 5*(1), 173–186.

van den Broeke, M., J. Bamber, J. Ettema, E. Rignot, E. Schrama, and B. Wouters (2009), Partitioning recent Greenland mass loss, *Science 326*, 984–986.

Velicogna, I. (2009), Increasing rates of ice mass loss from the Greenland and Antarctic ice sheets revealed by GRACE, *Geophys. Res. Lett. 36*, L19503. doi: 10.1029/2009GL040222.

Weidick, A., and E. Morris (1998), Local glaciers surrounding the continental ice sheets, in Into the Second Century of World-Wide Glacier Monitoring - Prospects and Strategies, edited by W. Haeberli et al., pp. 197–207, UNESCO, Paris.

WGMS (2008), Global glacier changes: Facts and figures, Zemp, M., Roer, I., Kääb, A., Paul, F., Hoelzle, M., Haeberli, W. pp. 88, UNEP/DIWA/GRID, Geneva.

Zwally, H., et al. (2002), ICESat's laser measurements of polar ice, atmosphere, ocean, and land, *J. Geodyn. 34*(3–4), 405–445.